Proc. Natl. Acad. Sci. USA
Vol. 94, pp. 3040–3045, April 1997
Cell Biology

The ultrastructural localization of 60-kDa Ro protein and human cytoplasmic RNAs: Association with novel electron-dense bodies

A. DARISE FARRIS*, FRANCINE PUVION-DUTILLEUL†, EDMOND PUVION†, JOHN B. HARLEY*, AND LELA A. LEE*‡

*Arthritis and Immunology Program, Oklahoma Medical Research Foundation, University of Oklahoma Health Sciences Center, and Department of Veterans Affairs Medical Center, Oklahoma City, OK 73104; and †Laboratoire Organisation Fonctionnelle du Noyau, Institut Fédératif Centre National de la Recherche Scientifique, Unité Propre de Recherche 9044, 94801, Villejuif Cedex, France

Communicated by Aaron B. Lerner, Yale University School of Medicine, New Haven, CT, December 10, 1996 (received for review April 8, 1996)

ABSTRACT **The 60-kDa Ro ribonucleoprotein is an important target of humoral autoimmune responses. However, the ultrastructural locations of the 60-kDa Ro protein and its associated small cytoplasmic RNAs (Y RNAs) have not been previously determined, and the functions of the Ro protein and RNAs are not known. In this study, the cellular locations of the 60-kDa Ro protein and the Ro Y1 and Y4 RNAs are determined by immunoelectron microscopy and *in situ* hybridization electron microscopy, respectively. Both Ro protein and Y RNAs are concentrated in discrete areas of the nucleoplasm, nucleolus, and cytoplasm of cultured cells and human skin sections. The 60-kDa Ro protein and Y RNAs are also present diffusely in the cytoplasm, where they occur in ribosome-rich regions, and in the nucleus. The presence of Ro ribonucleoprotein components in nucleoli and in ribosome-rich cytoplasmic areas suggests a potential for the involvement of Y RNAs and/or 60-kDa Ro protein in ribosome synthesis, assembly, or transport. Double labeling experiments show that Ro protein and Y RNAs colocalize in the nucleoplasm, nucleolus, and cytoplasm. In addition, aggregates of Y RNA occur unassociated with 60-kDa Ro protein, and aggregates of 60-kDa Ro protein occur unassociated with Y RNA. Aggregates of both Ro protein and Y RNAs label previously unreported nuclear and cytoplasmic electron-dense bodies. We propose that these distinctive Ro-associated electron-dense bodies may represent structure(s) important for cellular transport and/or Ro function.**

Ro ribonucleoproteins (RNP) were first identified as targets of humoral autoimmune responses in patients with systemic lupus erythematosus and Sjögren syndrome. Antibodies to 60-kDa Ro have been linked to specific subsets of lupus, including "ANA-negative" systemic lupus erythematosus, subacute cutaneous lupus erythematosus, homozygous C_2 deficiency with systemic lupus erythematosus, and neonatal lupus (1). In all of these subsets, photosensitive skin disease is a prominent finding, whereas internal organs are often minimally affected. It appears that the autoantibodies may play a causative role, since women who have anti-Ro may have babies with transient subacute cutaneous lupus skin lesions (2).

The Ro RNP family includes the 60-kDa Ro protein, which is associated with one of four human cytoplasmic RNAs (hY RNAs). Four distinct small cytoplasmic RNAs (Y RNAs) are immunoprecipitated from nucleated human cells with antibodies to 60-kDa Ro (hY1, hY3, hY4, and hY5); they range from 85 to 112 nucleotides in length and are products of RNA polymerase III transcription (3–6). Western blot analysis and DNA sequencing reveal a high conservation of the 60-kDa Ro protein among vertebrates, with a 78% identity between the human and *Xenopus* proteins (7, 8). Like the 60-kDa Ro protein, the 60-kDa Ro-associated Y RNAs are conserved among vertebrates by immunoprecipitation and by sequence, although the number of Y RNAs present is not conserved (3, 6, 8–14).

That the Ro RNP is highly conserved and is, in addition, present in every cell type tested suggests that it plays an important role in cellular metabolism. That role, however, remains unknown. Efforts to characterize the location of the Ro RNPs in cells have included numerous immunofluorescence studies that variably localized the 60-kDa Ro protein to the nucleus (15–17), the cytoplasm (6, 18), or both (7, 19). Biochemical fractionation studies have suggested that the majority of Ro protein and Y RNAs reside in the cytoplasm of cells (5, 8, 20). Although one such study found an exclusively cytoplasmic location for the Y RNAs and the Ro RNP, a substantial amount of Y RNA-free Ro protein was detected in the nucleus (21). More recent studies include different approaches to determine the subcellular localization of the Ro RNP components. Microinjection of 60-kDa Ro into the cytoplasm of *Xenopus* oocytes resulted in redistribution of the antigen to both the nucleus and the cytoplasm, whereas microinjection of hY1 RNA into oocyte nuclei resulted in redistribution to the cytoplasm (22). Overexpression of recombinant 60-kDa Ro cDNA in transfected HEp-2 cells resulted in a nuclear speckled immunofluorescence pattern with prominently stained nucleoli and weak cytoplasmic staining when reacted with anti-60-kDa Ro-specific antisera (23). A study of the subcellular localization of hY RNAs at the optical level by *in situ* hybridization to hY RNA-specific oligonucleotides resulted in the detection of all four hY RNAs in the cytoplasmic compartment, as well as detection of the hY1, hY3, and hY5 RNAs in the nuclear compartment, with concentrated staining in small areas near the periphery of nucleoli (24).

A speckled or particulate immunofluorescent staining pattern has been observed in studies detecting 60-kDa Ro both in the nucleus (referenced above) and cytoplasm (25) of cells, suggesting that the protein could be concentrated in small areas of the cell.

In this study, the subcellular localization of components of the Ro RNP has been examined by *in situ* hybridization electron microscopy and immune electron microscopy in an effort to identify unique ultrastructural features that may provide clues to the function of the Ro complex and/or its components. Both Y RNA and Ro protein are concentrated in small, discrete areas of the human cell cytoplasm, nucleoplasm, and nucleolus, in frequent association with novel subcellular particles we term "Ro-associated electron-dense bodies." These sites of Y RNA and Ro protein do colocalize in some but not all instances, suggesting that separate pools of Y RNA and Ro protein exist in cells, in addition to RNP particles containing Y RNA and Ro protein. The presence of Ro-associated electron-dense bodies in multiple cellular compartments, as well as at the nuclear membrane, suggest a possible role for the dense bodies in cellular transport. Although Y RNAs and Ro protein were not observed in coiled bodies, one site of

The publication costs of this article were defrayed in part by page charge payment. This article must therefore be hereby marked "*advertisement*" in accordance with 18 U.S.C. §1734 solely to indicate this fact.

0027-8424/97/943040-6$2.00/0
PNAS is available online at **http://www.pnas.org**.

Abbreviations: RNP, ribonucleoprotein; Y RNA, small cytoplasmic RNA that is associated with the 60-kDa Ro protein; hY RNA, human cytoplasmic RNA that is associated with the 60-kDa Ro protein.

‡To whom reprint requests should be addressed.

spliceosome component accumulation, they were found, in human skin, to label interchromatin granules, another site at which spliceosomal components concentrate. The detection of Ro RNP components in nucleoli and ribosome-rich cytoplasmic regions suggests a potential for the involvement of Y RNAs and/or Ro protein in ribosome synthesis, assembly, or transport.

METHODS

Cells and Specimen Preparation. HeLa and HEp-2 cells were cultured as monolayers in 5-cm plastic dishes. Before confluence, cell cultures were fixed in either 4% formaldehyde (Merck) or 1.6% glutaraldehyde (Taab Lab Equipment, Reading, U.K.) in 0.1 M Sorenson phosphate buffer (pH 7.3) for 1 h at 4°C. During the fixation, cells were detached from the plastic substrate and centrifuged. The pellets were washed for 2 h in the phosphate buffer, dehydrated in increasing concentrations of methanol, and embedded in Lowicryl K4M (26). Normal human neonatal keratinocytes obtained from circumcision were cultured in serum-free medium (27) and used at the second or third passage at ≈85% confluence. Keratinocytes were processed as above, except fixation was in either 1.6% or 0.8% glutaraldehyde. Normal human neonatal skin was collected immediately following circumcision and fixed in 1.6% glutaraldehyde or 4% formaldehyde as above. Polymerization of HeLa, HEp-2, and keratinocyte-embedded cells, as well as human skin, was carried out under long wavelength UV light (Philips fluorescence tubes TL 6W) for 5 days at −20°C and for 1 day at room temperature. Ultrathin sections were mounted on carbon-Formvar-coated gold grids (200 mesh).

Biotinylated Probes. The biotinylated probes used to detect Y RNAs were generated by nick-translation of pUC18 plasmids containing full-length Y cDNAs. Two micrograms of whole plasmid DNA was nick translated, incorporating biotin-11-dUTP (Sigma), with the GIBCO/BRL nick-translation system according to the manufacturer's instructions. Reactions were stopped by the addition of EDTA (pH 8.0) to a final concentration of 15 mM. Biotinylated DNA was recovered by ammonium acetate/ethanol precipitation in the presence 20 μg of carrier *Escherichia coli* genomic DNA. Three percent of the recovered DNA was electrophoresed in a 5% denaturing polyacrylamide gel, then electroblotted to nylon membrane. Biotinylated probe was detected with an avidin-alkaline phosphatase conjugate (Sigma), followed by development with nitro blue tetrazolium and 5-bromo-4-chloro-3-indolyl phosphate as described (28). Labeled fragments ranged from 100 to 1,000 nucleotides in size. The probes were redissolved and ethanol-precipitated twice more prior to resuspension in distilled water to a final concentration of about 60 μg/ml biotinylated DNA. Storage was at −20°C.

***In Situ* Hybridization.** Hybridization solutions contained 10 μg/ml either individual biotinylated probe or a mixture of all biotinylated probes, 50% deionized formamide, 10% dextran sulfate, 2× SSC (1× SSC = 0.15 M NaCl/0.015 M sodium citrate, pH 7), and 400 μg/ml *E. coli* DNA. Probes were denatured just prior to use by heating at 100°C for 4 min.

Grids bearing sections were floated for 3 h at 37°C on 2-μl drops of denatured hybridization solutions, rinsed over three drops (10 μl each) of PBS, and floated for 30 min over 5-μl drops of goat antibiotin immunoglobulins conjugated to gold particles, 10 nm in diameter (Biocell Research Laboratories, Cardiff, Wales), diluted 1:25 in PBS. After washing over three drops of PBS and a jet of distilled water, grids were stained for 10 min with 5% aqueous uranyl acetate. Some grids were placed in contact with the hybridization solutions following enzymatic treatments performed at 37°C and then processed for the detection of hybrids as described above. A 0.2 mg/ml protease pretreatment of sections (bacterial protease type VI; Sigma) for 15 min was performed to determine whether the accessibility of the probe to the target was affected by the presence of protein. An RNase pretreatment of sections [1 mg/ml RNase A (BDH) in 10 mM Tris·HCl buffer, pH 7.3] for 1 h was performed to evaluate the specificity of the hybridization signal.

A number of control experiments included the use of biotinylated human DNA probes specific for ribosomal RNA (provided by J. P. Bachellerie, Laboratoire de Biologie Moléculaire Eukaryote, Toulouse, France) and U1 and U2 small nuclear RNAs [provided by J. P. Bachellerie, J. E. Dahlberg (University of Wisconsin, Madison), and T. Pederson (Worcester Foundation for Experimental Biology, Shrewsbury, MA)], as well as a biotinylated poly(dT) probe (labeled by us) consisting of a synthetic polynucleotide with an average length of 171 nt (Pharmacia).

Anti-Ro Antibodies. Antiserum C is a patient antiserum positive for anti-Ro and anti-nRNP that has been affinity-purified for anti-Ro. This antiserum is one of a group of anti-Ro/anti-nRNP positive sera that recognizes 60-kDa Ro well in Western blot (29). For affinity purification, 10 mg of purified bovine Ro protein (30, 31) was coupled to 1 ml of preactivated Sepharose 4B (Sigma). After passing antiserum C over the column, the unretained fraction was reserved, whereas the retained fraction was eluted with 3 M sodium thiocyanate. The unretained fraction was concentrated, reapplied to the column, and eluted twice more. The resulting affinity-purified antiserum C was negative for anti-nRNP by RNA immunoprecipitation, Western blot, and ELISA; it was positive for anti-60-kDa Ro by RNA immunoprecipitation and Western blot analysis. Although whole serum recognized 52-kDa Ro on Western blot analysis, this recognition was undetectable following affinity purification. All experiments with antiserum C were performed with the affinity-purified material.

Antiserum A is a patient antiserum monospecific for 60-kDa Ro by ELISA, immunoblotting, RNA immunoprecipitation, and immunodiffusion. This serum is also negative for anti-52-kDa Ro by immunoblotting and ELISA.

Immunocytology. Grids bearing sections were floated on 5-μl drops of antibody C or A, diluted 1:50 and 1:10 in PBS, respectively, for 1 h at room temperature. After rapid washing on drops of PBS, grids were floated for 30 min over 5-μl drops of goat anti-human IgG conjugated to gold particles, 10 nm in diameter (Amersham), diluted 1:50 in PBS. After washing in a jet of distilled water, grids were stained for 10 min with 5% aqueous uranyl acetate. Unless otherwise indicated, sections were pretreated for 20 min at room temperature with normal rabbit serum (1:10 in PBS) and 5% BSA mixed 1:1 (vol/vol).

To demonstrate the specificity of labeling with antisera C and A, control experiments were performed by floating the grids for 1 h at room temperature over 5-μl drops of a mixture of purified bovine Ro protein and C or A antibody (1.6 μg of Ro protein plus 5 μl of 1:50 C antibody). These blocking conditions were first established in immunofluorescence studies. In addition, some grids were placed in contact with the immune sera following a protease pretreatment of sections performed as described above. A number of control experiments were undertaken, including the use of rabbit serum R288 directed against p80-coilin (provided by E. K. L. Chan and E. M. Tan, The Scripps Research Institute, La Jolla, CA) followed by anti-rabbit IgG conjugated to gold particles, 10 nm in diameter (Biocell Laboratories), and either anti-B36 mAb directed against fibrillarin (provided by M. E. Christensen, Georgetown College, Georgetown, KY) or anti-Sm Y12 mAb (provided by J. A. Steitz, Howard Hughes Medical Institute, New Haven, CT), each followed by anti-mouse antibody conjugated to gold particles, 10 nm in diameter (Biocell Laboratories).

Colocalization of hY RNA and Ro Protein. Grids bearing sections were first hybridized to a cocktail of hY probes (1, 3, 4, and 5) for 1 h at 37°C as described above. Following washing in PBS, the grids were then incubated in the presence of antiserum C (1:50 in PBS) for 1 h at room temperature as described above. Following washing in PBS, the grids were incubated in a mixture of rabbit anti-biotin antibody (Enzo Biochem) and anti-human IgG conjugated to gold particles, 10 nm in diameter (Amersham), for 30 min. The grids were once

again washed in PBS, then incubated in anti-rabbit IgG conjugated to gold particles, 5 nm in diameter (Biocell Laboratories), for 30 min. Following washing in PBS, the grids were stained with uranyl acetate as described above.

Electron Microscopy. Grids were observed in a Philips 400 electron microscope at 80 kV at magnifications between ×6,000 and ×22,000. Micrographs of glutaraldehyde-fixed cells originating from grids processed in parallel were used for quantitative evaluations of gold particle density following either *in situ* hybridization with biotinylated probes or immunogold labeling with anti-Ro antibodies. The areas of the various cell regions were measured using a Hewlett–Packard 9845B desktop computer interfaced with a 9111A graphic tablet. The number of gold particles within the measured areas was manually counted, and the density of labeling (number of gold particles per square micrometer) was calculated.

RESULTS

Detection of Ro RNAs in Cultured Cells. *In situ* hybridization was performed using a cocktail of biotinylated DNA probes for all four hY RNAs, and gold labeling was used to localize the binding of the probes. In cultured cells, gold labeling consisted of clusters of 8–80 gold particles present over the nucleus (Fig. 1) or cytoplasm, whereas a few individual gold particles were found scattered over the cells. In the nucleus, clusters were present mainly over the nucleoplasm, often adjacent to clusters of interchromatin granules. A few clusters were observed at the nuclear border, sometimes in association with masses of perinuclear condensed chromatin, and clusters were occasionally seen over the nucleolus. Labeling was excluded from the coiled bodies, the nuclear bodies, the clusters of interchromatin granules, and their associated zones (32–34). In the cytoplasm, clusters were observed over the ribosome-rich regions at variable distances from the nucleus and the plasma membrane. Other cytoplasmic organelles including mitochondria and the Golgi apparatus were entirely devoid of labeling. The distribution of the labeling and the frequency and size of the clusters of gold particles were unaffected by protease pretreatment of thin sections. RNase digestion of thin sections prior to hybridization, however, resulted in a total absence of labeling. Results were similar in all cell types.

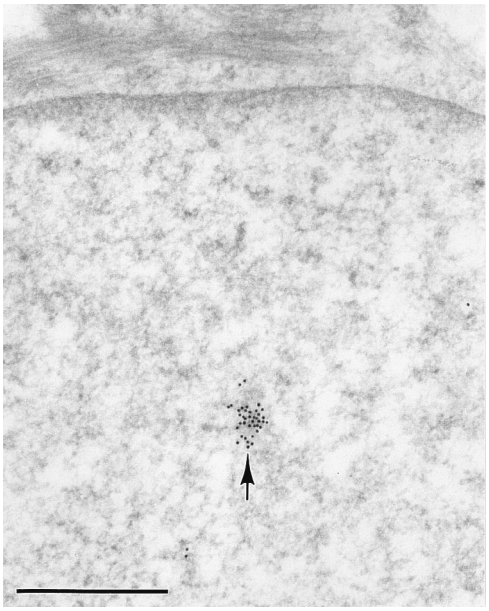

FIG. 1. Intranuclear localization of Ro RNA in a cultured keratinocyte by *in situ* hybridization with hY1 + hY3 + hY4 + hY5 probe mixture. A cluster of gold particles (10 nm) is present within the nucleoplasm. Glutaraldehyde fixation was 1.6%. Image produced by uranyl acetate staining. (Bar = 0.5 μm.)

Hybridization was also performed with individual hY RNA probes. The results using the hY1 and hY4 probes were similar to those using the cocktail of all four probes, although labeling with the hY4 probe was rarer than with either the hY1 or hY1 + hY3 + hY4 + hY5 probes. Hybridization with the hY3 probe was much less efficient yet still had the aspect of clusters. Hybridization with the hY5 probe was unsuccessful, possibly the result of unstable hybrid formation due to the short length of the complementary region of this probe. Therefore, the probes for the hY1 and hY4 RNAs are primarily responsible for the signals observed with the hY1 + hY3 + hY4 + hY5 probe cocktail.

Successful hybridizations with biotinylated probes to other cellular RNAs, including rRNAs, U RNAs, and poly(A)$^+$ RNAs, never gave labelings similar to the Y RNA probes, even when the experiments were performed in parallel.

Distribution of Ro Protein in Cultured Cells. Affinity-purified anti-Ro antibodies (antiserum C) were used to localize the Ro protein. Clusters of gold particles were observed in the nucleoplasm, in the cytoplasm, and occasionally at the nuclear border and in the nucleolus. Often, clustered labeling was present over small electron-dense bodies in the nucleoplasm, in the nucleolus, at the nuclear border (Fig. 2*A*), and in the cytoplasm (Fig. 2*B*) of all cell types tested. These labeled dense structures were round or ovoid in shape, typically 130–240 nm in diameter. Labeled electron-dense bodies were most easily and frequently observed in cultured keratinocytes.

In addition to clustered labeling, gold particles were also seen scattered over the cells. In the nucleus, scattered labeling was observed over the nucleoplasm and not over the clusters of interchromatin granules or their associated masses. In the cytoplasm, labeling was observed over the ribosome-rich areas, and mitochondria were devoid of labeling. Quantitative estimations performed on glutaraldehyde-fixed cells revealed that in most of the cells cytoplasmic labeling (6 ± 2 gold particles per μm^2) was more intense than nuclear labeling (3 ± 1 gold particles per μm^2).

Results obtained following the use of antiserum A were generally similar to those of antiserum C, with both clustered and diffuse labeling observed. However, labeling was generally

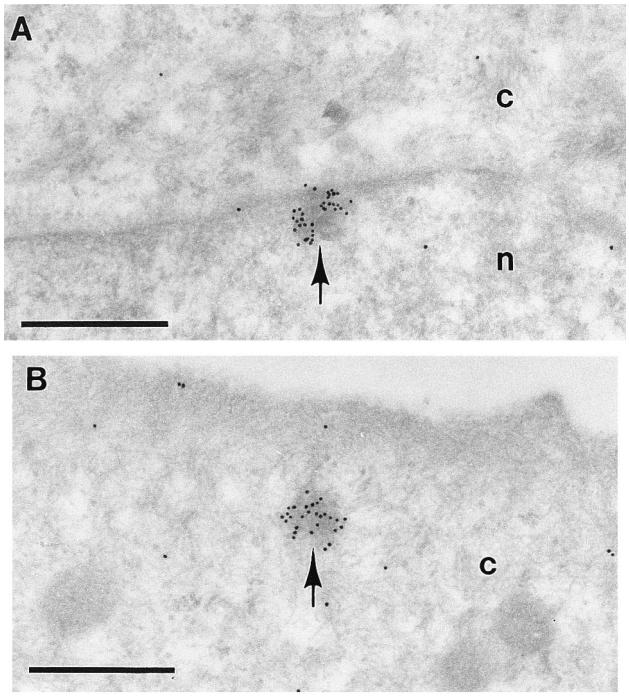

FIG. 2. Localization of Ro protein in cultured keratinocytes by immunogold labeling with antiserum C. Gold particles (10 nm) accumulate over electron-opaque bodies (arrows) at the nuclear border (*A*) and in the cytoplasm (*B*). c, Cytoplasm. Glutaraldehyde fixation was 1.6%. Image produced by uranyl acetate staining. (Bars = 0.5 μm.)

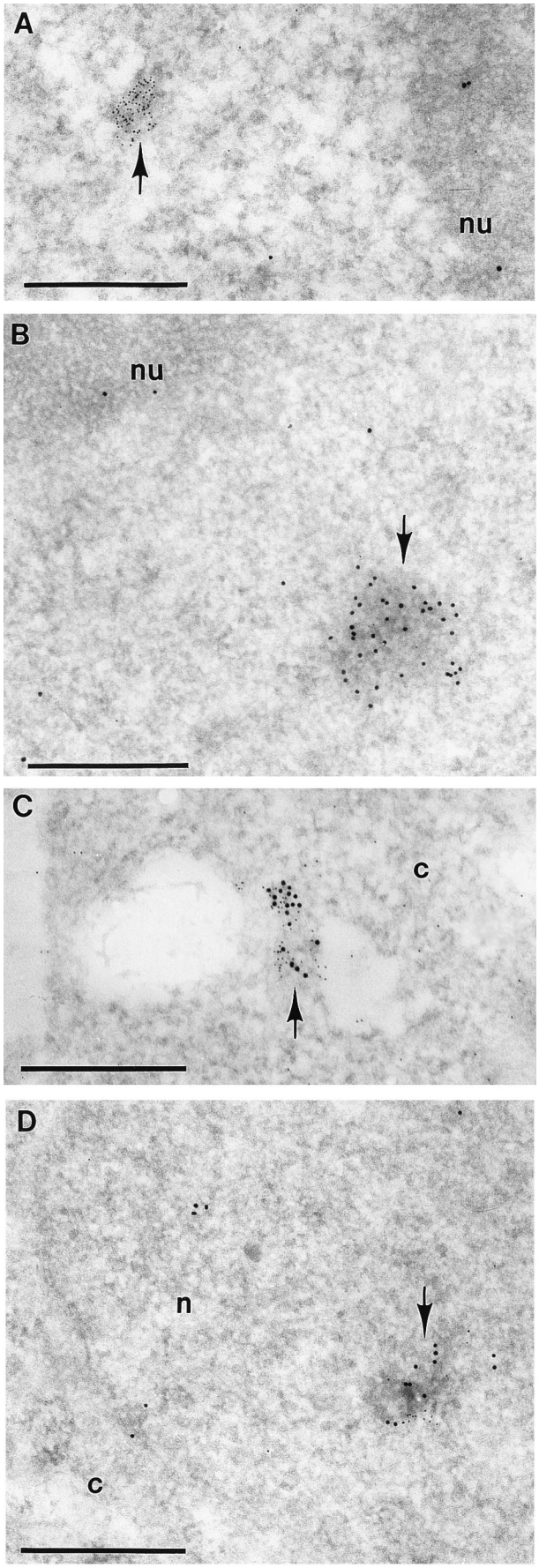

FIG. 3. Colocalization of hY RNA and Ro protein. Gold particles, 5 nm in diameter, label the hY RNA, whereas the 10-nm gold particles label the Ro protein. Formaldehyde fixation was 4%. Image produced by uranyl acetate staining. (*A*) Part of a nucleus of a HeLa cell. A cluster of 5-nm gold particles only (arrow) is observed within the nucleoplasm. Individual 5-nm and 10-nm gold particles are present. nu, nucleolus. (*B*) Part of a nucleus of a HEp-2 cell. A cluster of 10-nm gold particles only (arrow) labels an electron-opaque spot within the nucleoplasm in which individual 10-nm gold particles are scattered. nu, Nucleolus. (*C*) HEp-2 cell. A cluster of mixed 5-nm and 10-nm gold particles (arrow) is present in the cytoplasm (c). (*D*) HEp-2 cell. A cluster of mixed 5-nm and 10-nm gold particles (arrow) is present within the nucleoplasm over an electron-opaque spot, which appears as highly contrasted fibrils. c, Cytoplasm; n, nucleus. (Bars = 0.5 μm.)

weaker with antiserum A, and no preferential labeling of nuclear borders or nucleoli was observed. Since clustered labeling of these latter sites was infrequent with antiserum C, and since fewer total clusters were observed with antiserum A, the lack of nucleolar and nuclear border clusters with antiserum A could be due to differences in antibody titer, affinity, or avidity.

Sections stained with secondary antibody conjugate alone were entirely devoid of labeling. In addition, the gold labeling of HeLa and HEp-2 cells was reduced to near zero by preincubation of sera with purified Ro protein or by pretreatment of thin sections with protease. Although a few isolated gold particles were occasionally seen under these conditions, clusters of gold particles were never found. Immunocytology performed on control sections with antibodies to p80-coilin, fibrillarin, and Sm antigens gave the expected labelings, which did not resemble the observed Ro binding pattern.

Colocalization of hY RNA and Ro Protein in HeLa Cells. Double labeling of sections for hY RNA and Ro protein was accomplished by first hybridizing a cocktail of probes for hY1 + hY3 + hY4 + hY5 RNAs with sections of HeLa cells, then subsequently incubating the sections with antiserum C. Binding was revealed by immunocytology, with Y RNA hybrids being labeled with 5-nm gold particles and Ro protein with 10-nm gold particles. Control experiments conducted by labeling sections with secondary antibody and antibody/gold conjugates alone resulted in an absence of labeling.

Clusters of gold particles, either 5 nm only (RNA clusters, Fig. 3*A*) or 10 nm only (protein clusters, Fig. 3*B*), were present in the nucleus and in the cytoplasm. Clusters of 5-nm and 10-nm gold particles showing the same localization (RNA–protein clusters, Fig. 3 *C* and *D*) were also observed in the nucleoplasm, at the nuclear border, in the nucleolus, and in the cytoplasm. Some RNA–protein clusters consisted of primarily either 5-nm or 10-nm gold particles, whereas others contained about the same proportion of the two sizes of gold particles. The former observation suggested that antigenic sites of the Ro protein could be hidden by the already bound probes. Therefore, sections were incubated with antiserum C prior to the hybridization step. This protocol did not significantly modify the labeling. Thus, it would appear that probe hybridization to Y RNAs did not shield Ro protein epitopes. Clusters, both mixed and those composed of only 10-nm gold particles, were often over electron-dense bodies in both the cytoplasm and the nucleus. In addition to clustered labeling, isolated gold particles 10 nm in diameter and, to a lesser extent, 5 nm in diameter were randomly scattered throughout the cells.

Ro Y RNA and Protein Localization in Human Skin. To assess whether the Ro RNA and protein localization patterns observed in cultured cells were also present in normal, uncultured cells, *in situ* hybridization and immunocytology were performed on sections of fixed and embedded fresh human skin. Upon *in situ* hybridization with probes for the hY1 + hY3 + hY4 + hY5 RNAs, clusters of 5–35 gold particles were seen in the nucleoplasm, the cytoplasm, at the nuclear border, and occasionally in the nucleolus, where clusters were observed near the nucleolar periphery (Fig. 4). Scattered individual or groups of 2 or 3 gold particles were seen throughout the cells, including the intranuclear clusters of interchromatin granules.

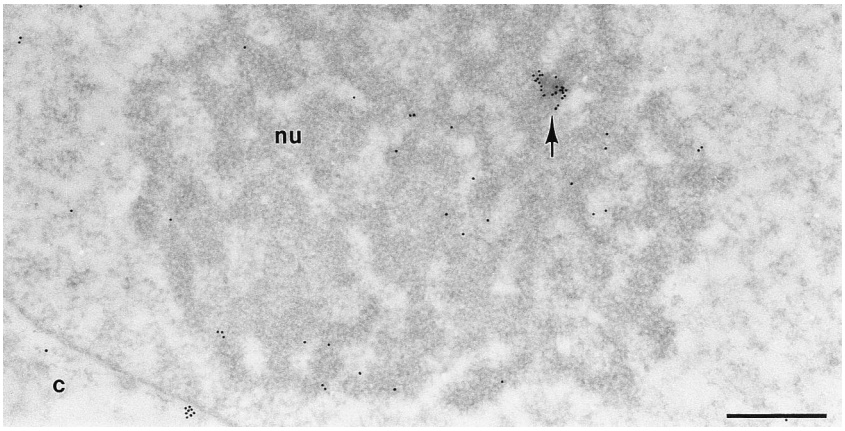

FIG. 4. Intranuclear localization of Ro RNA in skin by *in situ* hybridization with hY1 + hY3 + hY4 + hY5 probe mixture. A cluster of gold particles (10 nm; arrow) is located at the periphery of the nucleolus (nu) in association with a portion of its fibrillar component, whereas individual gold particles are scattered through the cell. Formaldehyde fixation was 4%. Image produced by uranyl acetate staining. (Bar = 0.5 μm.)

Using affinity-purified antibody to identify Ro protein, clusters of gold particles were once again seen in both the nucleus and cytoplasm and at the nuclear border, on both the nucleoplasmic and cytoplasmic faces of the nuclear membrane (Fig. 5). Scattered individual gold particles were also seen in the nucleus and cytoplasm of cells, at a frequency similar to that seen with *in situ* hybridization of skin sections (9 ± 2 and 10 ± 2 gold particles per μm^2 of nuclear and cytoplasmic compartments, respectively, of glutaraldehyde-fixed cells). In contrast to cultured cells and similarly to skin sections labeled with hY1 + hY3 + hY4 + hY5 probe cocktail, individual gold particles were present over the clusters of interchromatin granules (Fig. 5). Results were similar with antiserum A, although labeling was less frequent. In addition, labeling was blocked by preincubation of antibodies or serum with purified Ro protein.

Clustered labeling observed in skin sections by both *in situ* hybridization and immunoelectron microscopy was frequently over electron-dense bodies similar in size and appearance to those labeled in cultured cells. That dense bodies were readily labeled by Y RNA probe cocktail in thin sections of skin is in contrast to results from cultured cells, where detection of Y RNA containing dense bodies with Y RNA probe cocktail was rare.

DISCUSSION

In situ hybridization electron microscopy and immunoelectron microscopy has allowed detection of Ro RNP components at high resolution using thin sections of Lowicryl-embedded cells. Although this technique allows only those antigenic sites exposed at the cut surface of the sections to be revealed (35), excellent hybridization specificity as well as good structural preservation is routinely obtained (32).

Human Y1 and Y4 RNAs detected by *in situ* hybridization in three different cell lines and in human skin are found concentrated in discrete areas within the cytoplasm and the nucleus. Within the nucleus, Y RNAs are clustered in the nucleolus and in the nucleoplasm but are not associated with known nuclear structures such as coiled bodies, nuclear bodies, interchromatin granules, or their associated zones. In skin, however, individual gold particles are scattered over the interchromatin granules. This indicates that at least in some cases clusters of interchromatin granules may contain significant amounts of Y RNAs. Since the clusters of interchromatin granules are known to contain small nuclear RNAs (32), poly(A)$^+$ RNAs (33), and ribosomal RNAs (36), in addition to spliceosomal components, the occasional detection of Y RNAs in these structures suggests that interchromatin granules might be storage or sorting sites for several RNA species. Although it is possible that the apparent exclusion of Ro protein and Y RNAs from interchromatin granules in cultured cells could have been due to sampling error, the absence of labeling of interchromatin granules in cultured cells more likely reflects a biological difference between cultured cells and normal tissue. In agreement with a recent study of Y RNA cellular localization at the optical level (24), Y RNAs localized in discrete areas within nucleoli near the nucleolar periphery and also to perinucleolar sites. Some of these sites may correspond to the perinucleolar compartment identified at the optical level in that study.

Immunoelectron microscopy with anti-Ro-specific antisera, which recognize determinants on the 60-kDa Ro protein, also resulted in the detection of Ro protein in small, discrete areas of the nucleus, including the nucleolus, and the cytoplasm. This discrete binding, which was frequently associated with small, electron-dense cellular bodies, occurred in addition to the

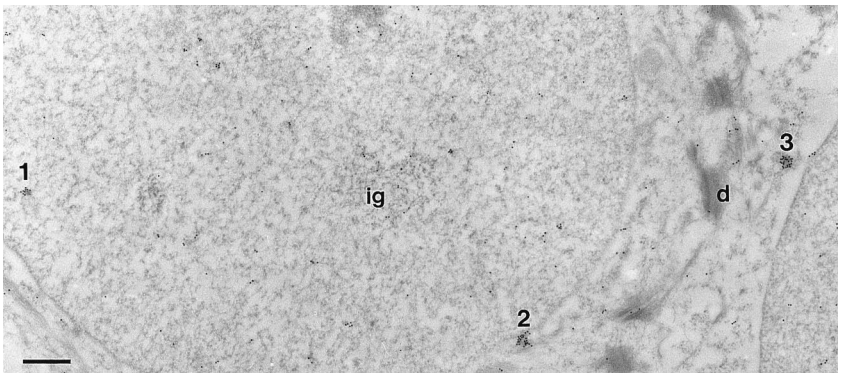

FIG. 5. Localization of Ro protein in skin by immunogold labeling with antiserum C. Isolated gold particles (10 nm) are scattered through the cell, including the cluster of interchromatin granules (ig) but excluding the desmosomes (d). In addition, clusters of gold particles (10 nm) are present within the nucleoplasm (1), at the nuclear border (2), and in the juxtanuclear cytoplasm (3) in association with electron-opaque bodies. Formaldehyde fixation was 4%. Image produced by uranyl acetate staining. (Bar = 0.5 μm.)

presence of significant labeling that was scattered throughout the cells. In skin, nonaggregated Ro protein was also localized within the clusters of interchromatin granules, a nuclear compartment in which spliceosome components accumulate.

The accuracy of Y RNA and 60-kDa Ro protein detection was confirmed by colocalizing Y RNA and Ro protein upon simultaneous *in situ* hybridization and immunoelectron microscopy. Interestingly, however, only subsets of the Y RNA and Ro protein pools could be localized to the same sites in cells, and this result cannot be explained by competitive binding since the order of detection procedures for RNA or protein did not significantly alter the results. These pools of non-colocalized Y RNA or Ro protein, which may not be components of Ro RNP complexes, were detected in both the nucleus and the cytoplasm. This is in partial agreement with others who have found pools of 60-kDa Ro protein not associated with Y RNAs (21, 22) and, conversely, pools of Y RNAs not associated with Ro protein (24) in the nucleus.

The presence of Ro protein in the nucleoplasm and Ro RNA in the cytoplasm of cells is likely to be functionally significant since these molecules must be relocated to these sites following their syntheses. However, the functions of the Ro protein and its associated Y RNAs have not been established. Since Ro protein binds mutant 5S rRNA precursors from frog oocytes, it has been suggested that uncomplexed nuclear Ro protein participates in the degradation of these mutant RNAs (37). Our data are not inconsistent with a transport model constructed from frog oocyte microinjection data in which Ro protein is relocated to the nucleus following translation, then, upon association with Y RNA, is quickly transported back to the cytoplasm as a RNP complex (22). If this model is correct, our data would further suggest that (*i*) once present in the cytoplasm, Ro RNP complexes can dissociate, and (*ii*) Ro RNPs assembled in the nucleoplasm might also be transported to the nucleolus.

That Ro RNP components and Ro-associated dense bodies localize to the nucleolus suggests a function for Ro in this compartment, such as ribosome assembly or transport. Although presumed Ro complexes are detected in the nucleolus by colocalization, it is still unclear whether uncomplexed Ro protein and RNA occur in this compartment, which could indicate dissociation of the RNP complex at this site. The answer to this question may be yes if perinucleolar compartments containing uncomplexed Y RNAs are within the nucleolus itself, as they appeared to be at the optical level (24).

Clustered labeling was often over electron-dense spots, which we call Ro-associated dense bodies, in both the nucleus and the cytoplasm, whether labeling detected Ro protein alone or colocalized Y RNA and Ro protein. Although we did not detect an association of uncomplexed Y RNAs with dense bodies, further study is needed to determine whether uncomplexed Y RNAs are clearly not associated with these structures. Although the significance of the electron-dense bodies labeled in the current study is uncertain, they could be Ro RNP-specific cellular structures, analogous to the nuclear structures known to accumulate spliceosome components (clusters of interchromatin granules, their associated zones, and coiled bodies) (35, 38, 39). On the other hand, although morphologically well identifiable typical nuclear bodies were always unlabeled, another possibility would be that the nuclear Ro-containing discrete domains might correspond to a specific subset of simple nuclear bodies (40, 41). The latter possibility is less likely since morphologically similar cytoplasmic structures are also labeled by Ro RNP components. It seems more likely that Ro-associated dense bodies are shuttled between the different compartments, functioning primarily either in the storage and transport of Ro components or in the transport of other macromolecules.

To our knowledge, this is the first report describing Ro RNP localization at the electron microscopic level as well as the first one to examine Y RNA localization in human keratinocytes and skin. The results of this study suggest that the Ro RNP and components of the Ro RNP complex are concentrated in discrete areas of the nucleoplasm, the nucleolus, and the cytoplasm of cells and may be seen in association with a novel subcellular particle we have termed the Ro-associated electron-dense body. These findings may explain, at the ultrastructural level, the speckled or particulate Ro-associated immunofluorescent staining patterns seen with visible fluorescence in both the cell nucleus (15–17, 23) and cytoplasm (25). Purification and characterization of the novel Ro-associated dense bodies, including identification of any other colocalizing molecules, should provide insight into Ro RNP function.

We thank Kathleen Alvarez, Timothy Gross, and Evelyne Pichard for their valuable technical assistance. We thank E. K. L. Chan and E. M. Tan, M. E. Christensen, and J. A. Steitz for their gifts of control antibodies used in this study. We also thank J. P. Bachellerie, J. E. Dahlberg, and T. Pederson for gifts of RNA-encoding plasmids and biotinylated probes, which were used as controls in this study. This work was funded in part by grants from the U.S. Department of Veteran's Affairs, the Oklahoma Center for Molecular Medicine, and the National Institutes of Health (AI31584, AR42460, AR42474, and AI24717). This work was also funded by the Centre National de la Recherche Scientifique and by special grants from the Association pour la Recherche sur le Cancer (Villejuif, France) and the Ligue Nationale contre le Cancer (Paris). F.P.-D. is a member of the Institut National de la Santé et de la Recherche Médicale.

1. Reichlin, M. (1986) *J. Clin. Immunol.* **6,** 339–348.
2. Lee, L. A., Frank, M. B., McCubbin, V. R. & Reichlin, M. (1994) *J. Invest. Dermatol.* **102,** 963–966.
3. Wolin, S. L. & Steitz, J. A. (1983) *Cell* **32,** 735–744.
4. O'Brien, C. A. & Harley, J. B. (1990) *EMBO J.* **9,** 3683–3689.
5. Kato, N., Hoshino, H. & Harada, F. (1982) *Biochem. Biophys. Res. Commun.* **108,** 363–370.
6. Hendrick, J. P., Wolin, S. L., Rinke, J., Lerner, M. R. & Steitz, J. A. (1981) *Mol. Cell. Biol.* **1,** 1138–1149.
7. Slobbe, R. L., Pruijn, G. J. M., Damen, W. G., van der Kemp, J. W. & van Venrooij, W. J. (1991) *Clin. Exp. Immunol.* **86,** 99–105.
8. O'Brien, C. A., Margelot, K. & Wolin, S. L. (1993) *Proc. Natl. Acad. Sci. USA* **90,** 3683–3689.
9. Mamula, M. J., O'Brien, C. A., Harley, J. B. & Hardin, J. A. (1989) *Clin. Immunol. Immunopathol.* **52,** 435–446.
10. Craft, J., Mamula, M., Ohosone, Y., Boire, G., Gold, H. & Hardin, J. A. (1990) *Clin. Rheumatol.* **9,** 10–19.
11. Reddy, R., Tan, E. M., Henning, D., Nohga, K. & Busch, H. (1983) *J. Biol. Chem.* **258,** 1383–1386.
12. Itoh, Y., Kriet, J. D. & Reichlin, M. (1990) *Arthritis Rheum.* **33,** 1815–1821.
13. Farris, A. D., O'Brien, C. A. & Harley, J. B. (1995) *Gene* **154,** 193–198.
14. Van Horn, D. J., Eisenberg, D., O'Brien, C. A. & Wolin, S. L. (1995) *RNA* **1,** 293–303.
15. Harmon, C. E., Deng, J.-S., Peebles, C. L. & Tan, E. M. (1984) *Arthritis Rheum.* **27,** 166–173.
16. Wermuth, D. J., Geoghegan, W. D. & Jordan, R. E. (1985) *Arch. Dermatol.* **121,** 335–338.
17. Xia, P., Fritz, K. A., Geoghegan, W. D. & Jordan, R. E. (1987) *J. Clin. Lab. Immunol.* **22,** 101–105.
18. Bachmann, M., Mayet, W. J., Schröder, H. C., Pfeifer, K., zum Büschenfelde, K.-H. M. & Müller, W. E. G. (1986) *Proc. Natl. Acad. Sci. USA* **83,** 7770–7774.
19. Kelekar, A., Saitta, M. R. & Keene, J. D. (1994) *J. Clin. Invest.* **93,** 1637–1644.
20. Boire, G. & Craft, J. (1990) *J. Clin. Invest.* **85,** 1182–1190.
21. Peek, R., Pruijn, G. J. M., van der Kemp, A. J. W. & van Venrooij, W. J. (1993) *J. Cell Sci.* **106,** 929–935.
22. Simons, F. H. M., Pruijn, G. J. M. & van Venrooij, W. J. (1994) *J. Cell Biol.* **125,** 981–988.
23. Keech, C. L., McCluskey, J. & Gordon, T. P. (1994) *Clin. Immunol. Immunopathol.* **73,** 146–151.
24. Matera, A. G., Frey, M. R., Margelot, K. & Wolin, S. L. (1995) *J. Cell Biol.* **129,** 1181–1193.
25. Lee, L. A., Harmon, C. E., Huff, J. C., Norris, D. A. & Weston, W. L. (1985) *J. Invest. Dermatol.* **85,** 143–146.
26. Roth, J. (1989) in *Methods in Cell Biology*, ed. Tartakoff, A. M. (Academic, New York), pp. 513–551.
27. Boyce, S. T. & Ham, R. G. (1983) *J. Invest. Dermatol.* **81,** 33S–40S.
28. Boyle, A. (1993) in *Current Protocols in Molecular Biology*, eds. Ausubel, F. M., Brent, R., Kingston, R. E., Moore, D. D., Seidman, J. G., Smith, J. A. & Struhl, K. (Greene/Wiley, New York), pp. 3.18.4–3.18.5.
29. Rader, M. D., Codding, C. & Reichlin, M. (1989) *Arthritis Rheum.* **32,** 1563–1571.
30. Mamula, M. J., Fox, O. F., Yamagata, H. & Harley, J. B. (1986) *J. Exp. Med.* **86,** 1889–1901.
31. Scofield, R. H., Dickey, W. D., Jackson, K. W., James, J. A. & Harley, J. B. (1991) *J. Clin. Immunol.* **11,** 378–388.
32. Visa, N., Puvion-Dutilleul, F., Bachellerie, J. P. & Puvion, E. (1993) *Eur. J. Cell Biol.* **60,** 308–321.
33. Visa, N., Puvion-Dutilleul, F., Harper, F., Bachellerie, J. P. & Puvion, E. (1993) *Exp. Cell Res.* **208,** 19–24.
34. Puvion-Dutilleul, F., Besse, S., Chan, E. K. L., Tan, E. M. & Puvion E. (1995) *J. Cell Sci.* **108,** 1143–1153.
35. Puvion, E., Viron, A., Assens, C., Leduc, E. H. & Jeanteur, P. (1984) *J. Ultrastruc. Res.* **87,** 180–189.
36. Besse, S. & Puvion-Dutilleul, F. (1996) *J. Cell Sci.* **109,** 119–129.
37. O'Brien, C. A. & Wolin S. L. (1994) *Genes Dev.* **8,** 2891–2903.
38. Fakan, S., Leser, G. & Martin, T. E. (1984) *J. Cell Biol.* **98,** 358–363.
39. Spector, D. L. (1993) *Curr. Opin. Cell Biol.* **5,** 442–447.
40. Brasch, K. & Ochs, R. (1992) *Exp. Cell Res.* **202,** 211–223.
41. Koken, M. H. M., Puvion-Dutilleul, F., Guillemin, M. C., Viron, A., Linares-Cruz, G., Stuurman, N., de Jong, L., Szostecki, C., Calvo, F., Chomienne, C., Degos, L., Puvion, E. & de Thé, H. (1994) *EMBO J.* **13,** 1073–1083.